Journal of Volcanology and Geothermal Research 447 (2024) 108012

Contents lists available at ScienceDirect

Journal of Volcanology and Geothermal Research

journal homepage: www.journals.elsevier.com/journal-of-volcanology-and-geothermal-research

CO_2 budget from a 3D chemical tomography of a degassing volcanic lake (Lagoa das Furnas, São Miguel, Azores)

Giancarlo Tamburello [a,*], Dmitri Rouwet [a], César Andrade [b], Fátima Viveiros [b,c], J. Virgílio Cruz [b,c]

[a] Istituto Nazionale di Geofisica e Vulcanologia, Sezione di Bologna, Viale Berti Pichat 6/2, Bologna, Italy
[b] IVAR — Instituto de Investigação em Vulcanologia e Avaliação de Riscos, Universidade dos Açores, Rua Mãe de Deus, Edifício do Complexo Científico, 3° Andar - Ala Sul, Ponta Delgada 9500-321, Portugal
[c] FCT — Faculdade de Ciências e Tecnologia, Universidade dos Açores, Ponta Delgada, Portugal

ARTICLE INFO

Keywords:
Volcanic lake
Dissolved CO_2
Chemical tomography
CO_2 budget
Volcanic hazard

ABSTRACT

We here present a 3D mapping of the dissolved CO_2 at Lagoa das Furnas (São Miguel Island, Azores) obtained with an infrared-based probe that measures the partial pressure of CO_2 gas dissolved in liquids, and a multi-parametric probe to measure pH, ORP, conductivity, dissolved O_2, and temperature. We interpolated the dissolved CO_2 at different depths and around the lake to calculate the total mass of CO_2 dissolved as $CO_{2\,(aq)}$ (109–176 tons). We identified different plumes of dissolved CO_2 that spatially correspond to previously detected shallow anomalies of the diffusive CO_2 degassing at the water-air (interface) and hydroacoustic signatures of the bubbling activity. Our result represents the first direct quantification of the total dissolved CO_2 in a volcanic lake, opening new perspectives for volcanic lake monitoring and related hazard assessment.

1. Introduction

Degassing of CO_2 at volcanic lakes is mainly linked to the sudden and potentially fatal "Nyos-type" gas release, i.e. by lake rollover upon CO_2 supersaturation in deep lake strata, or upon an external trigger (e.g. earthquake, landslide) (Sigurdsson et al., 1987; Kling et al., 1987; Kusakabe, 2015, 2017). Nevertheless, as CO_2 is the most abundant dry gas species at degassing volcanoes – from purely magmatic to hydrothermal systems – a myriad of alternative degassing mechanisms is possible, depending on the physical-chemical characteristics of the lake the gas is flushing through: (1) acid crater lakes (pH < 3.4) topping the most active volcanoes are chemically transparent to CO_2, which will be released from the lake surface *tal qual* as it enters at the lake bottom (Rouwet et al., 2014; Tamburello et al., 2015; Shinohara et al., 2015; de Moor et al., 2016; Gunawan et al., 2017; Battaglia et al., 2019), (2) hyper-acid (pH < 2) and hyper saline crater lakes affected by high seasonal rainfall can "coat" the lake surface by cold, less dense and less acid waters to create CO_2 accumulation under its "skin" to eventually be hazardously released as a gas *beracun* (e.g. Kawah Ijen, Caudron et al., 2017; Rouwet, 2021), (3) shallow lakes, regardless of their pH, do not generate a sufficiently high hydrostatic pressure to keep the CO_2 dissolved, and (4) lakes in temperate regions, regardless of their depth, pair CO_2 release with density driven lake roll over in winter (Chiodini et al., 2012). As CO_2 is denser than air and hence tends to accumulate in depressions, a massive gas release can become hazardous in any of the above-mentioned release mechanisms.

The CO_2 efflux has been measured with the floating accumulation chamber method at many lakes worldwide (Mazot et al., 2011; Pérez et al., 2011; Jácome-Paz et al., 2015; Andrade et al., 2016, 2019; Melián et al., 2021), but the mechanism and velocity of CO_2 migration from bottom to top through a lake water body remains poorly constrained. Moreover, echo-sounding surveys at volcanic lakes with various acidities enabled localising the degassing vents and rising gas flares (Caudron et al., 2012; Hernández et al., 2017, 2021; Jolie, 2019), also on the study object of this study, Lagoa das Furnas, São Miguel Island, Azores (Melián et al., 2017).

Here we scrutinize the generally accepted assumption of horizontally homogeneous layering and CO_2 distribution in the water body of a volcanic lake. The proposed novel method is a 3D chemical tomography, probing the lake at various depths and sites, to obtain a snapshot 3D distribution of temperature, pH, electrical conductivity, redox state (Eh, dissolved O_2) and, especially, dissolved CO_2. The data are compared to

* Corresponding author.
E-mail address: giancarlo.tamburello@ingv.it (G. Tamburello).

https://doi.org/10.1016/j.jvolgeores.2024.108012
Received 26 October 2023; Received in revised form 15 January 2024; Accepted 17 January 2024
Available online 24 January 2024

the diffusive CO_2 degassing previously measured at the water-air interface. Lagoa das Furnas is particularly suited for this first test for being a shallow, relatively large lake with a clear manifestation of bubbling degassing from an adjacent and underlying hydrothermal system (Andrade et al., 2016).

2. Lagoa das Furnas

Lagoa das Furnas crater lake is located inside the more recent caldera of Furnas Volcano (10–12,000 years old, Guest et al., 2015), the easternmost of the three active central volcanoes that dominate the geology of São Miguel Island (Fig. 1a-b). The caldera is characterised by fault systems trending WNW–ESE, NE–SW, N—S and NNW–SSE. A minor WNW–ESE-oriented fault system is observed in Lagoa das Furnas margins (Carmo et al., 2015). The lake has a surface area of 1.87 km^2 and is elongated in an NNE-SSW direction (maximum length and width of 2025 m × 1600 m). The maximum depth recorded is ~15 m in the central-north sector (Andrade et al., 2016), but this depth may vary over time for the intra-annual and inter-annual fluctuations associated with climatic variability (Cruz et al., 2006). Furnas' volcanic activity is mainly related to four hydrothermal fumarolic fields that emit an H_2O-CO_2 rich gas mixture with minor H_2S, H_2, N_2, He, Ar, CH_4 and CO (Caliro et al., 2015), thermal and cold CO_2-rich springs, and diffusive CO_2 emissions from both lake and soil (1082–1630 $t{\cdot}d^{-1}$, Viveiros et al., 2010; Andrade et al., 2016, 2021). Subaqueous fumaroles at the northern shoreline produce visible bubbling at the water surface. Other deeper fumaroles have been localized with an echo sounder in the central western sector with no bubbling at the water-air interface. Probably the gas dissipates by dissolution before reaching the surface (Melián et al., 2017).

The isotopic composition of the dissolved CO_2 in the lake (Andrade et al., 2021) reveals two main sources: i) a biogenic source from the degradation of organic matter accumulated at the bottom of the lake ($\delta^{13}C \sim -17.42$ ‰ in the southern part), ii) a volcanic/hydrothermal source ($\delta^{13}C$ -1.94 – −7.18 ‰) observed in the CO_2 degassing zones, which composition encompasses the pure hydrothermal CO_2 end-member represented by the $\delta^{13}C$ of the gases emitted by the subaerial Furnas fumarolic field fumaroles (−4.21 ‰, Caliro et al., 2015). Nevertheless, the passive CO_2 degassing at the surface (Brumberg et al., 2021) and intense photosynthesis (Herczeg and Fairbanks, 1987) may also affect the isotopic composition of the dissolved CO_2.

3. Methodology

We used two probes to measure the water physicochemical properties of Lagoa das Furnas. The Pro Oceanus mini-CO_2 probe is an infrared detector hosted in a cylindrical (length 28 cm, diameter 5.3 cm) acetal plastic body that measures the partial pressure of CO_2 gas dissolved in liquids (pCO_2 range 10^2–$5{\cdot}10^4$ µatm, accuracy ±2% of max range, resolution 0.1% of max range). The measurement requires a certain amount of time for the equilibration between the CO_2 inside the probe and the dissolved CO_2 separated by a hydrophobic membrane. The T_{63} of the probe is ~3 min and indicates how long the measurement takes to reach 63% of the final value when there is an instant change in the variable. T_{63} is equal to the time constant for physical systems that behave exponentially under a sudden change, as for dissolved gas measurements.

The mini-CO_2 probe has an internal battery and data logger and can reach 600 m in depth.

The equilibrated ratio of partial pressure to dissolved concentration ($CO_{2(aq)}$ in $mol{\cdot}kg^{-1}$) is governed by Henry's law of solubility and its constant K_H typical for each gas. Weiss (1974) suggests that for total

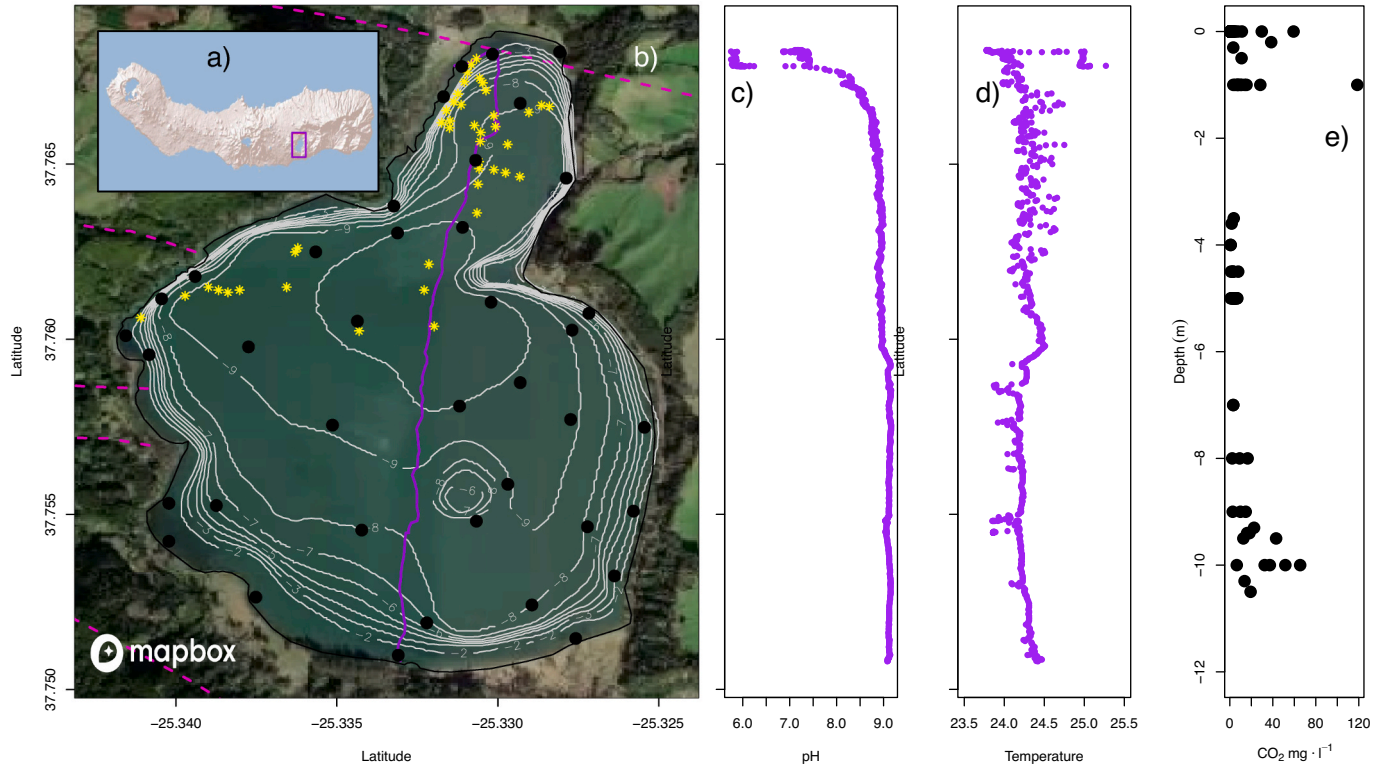

Fig. 1. a) São Miguel Island and location of Lagoa das Furnas. b) Satellite map of Lagoa das Furnas (Mapbox ©) with its bathymetry and the location of the main tectonic structures (magenta dashed lines, Guest et al., 2015; Carmo, 2013). Yellow stars show the position of the fumaroles and bubbling identified by Melián et al. (2017). Black circles show the sampling sites of this work. Purple lines and circles show the longitudinal transect with the measurements of pH and temperature (c and d). e) Plot of all the $CO_{2(aq)}$ measurements carried out at different depths and sites of the lake with the Pro-Oceanus probe. (For interpretation of the references to colour in this figure legend, the reader is referred to the web version of this article.)

pressures near 1 atm, CO_2 solubility can be written as follows:

$$\left[CO_{2(aq)}\right] = K_O \cdot pCO_2 \quad (1)$$

Where K_O ($mol \cdot kg^{-1} \cdot atm^{-1}$) is a solubility coefficient that is a function of both the temperature and the salinity of the water, through the relationship from Weiss (1974):

$$ln\,(K_O) = -60.2409 + 93.4517 \cdot \left(100 \cdot T^{-1}\right) + 23.3585 \cdot ln(0.01 \cdot T) + S\left(0.023517 - 0.023656 \cdot (0.01 \cdot T) + 0.0047036 (0.01 \cdot T)^2\right). \quad (2)$$

Where T is the temperature (Kelvin), and S the salinity (‰, approximately equal to PSU). For non-saline waters, the fourth term of the equation becomes zero, leading to.

$$ln\,(K_O) = -60.2409 + 93.4517 \cdot \left(100 \cdot T^{-1}\right) + 23.3585 \cdot ln \cdot (T \cdot 0.01) \quad (3)$$

Hence, we use Eqs. (1 and 3) to convert the measured CO_2 partial pressure into dissolved CO_2 concentration.

The Hanna Instrument HI9829 multiparametric probe hosts an integrated GPS system and an autonomous sensor for measuring pH, conductivity, redox potential, dissolved oxygen and temperature on a 20 m cable, hence not representing depth limitations for the case of Lagoa das Furnas.

A small boat was used to reach each point of measurement. The HI9829 probe was stationed at a constant depth every 2 m for a few minutes. The mini-CO_2 was stationed with a rope at three different depths (shallow, midpoint, bottom) for a more extended period (10–15 min, due to its slower response time) depending on the maximum depth of the measurement point. Following the work of Andrade et al. (2016), we selected the sampling points across the significant degassing anomalies and the non-degassing areas to obtain a quasi-regular grid. We localized 19 points offshore and 15 points near-shore around the lake coast. We also carried out transects at shallow depths (1–2 m) at a higher sampling rate across the two main fumarolic bubbling areas in the northern part of Lagoa das Furnas and along the central axis of the lake. Additionally, we carried out a longitudinal north-south transect with a kayak and the HI9829 probe submerged at 1-m depth to explore the shallow variability of the physical-chemical parameters at high spatial resolution.

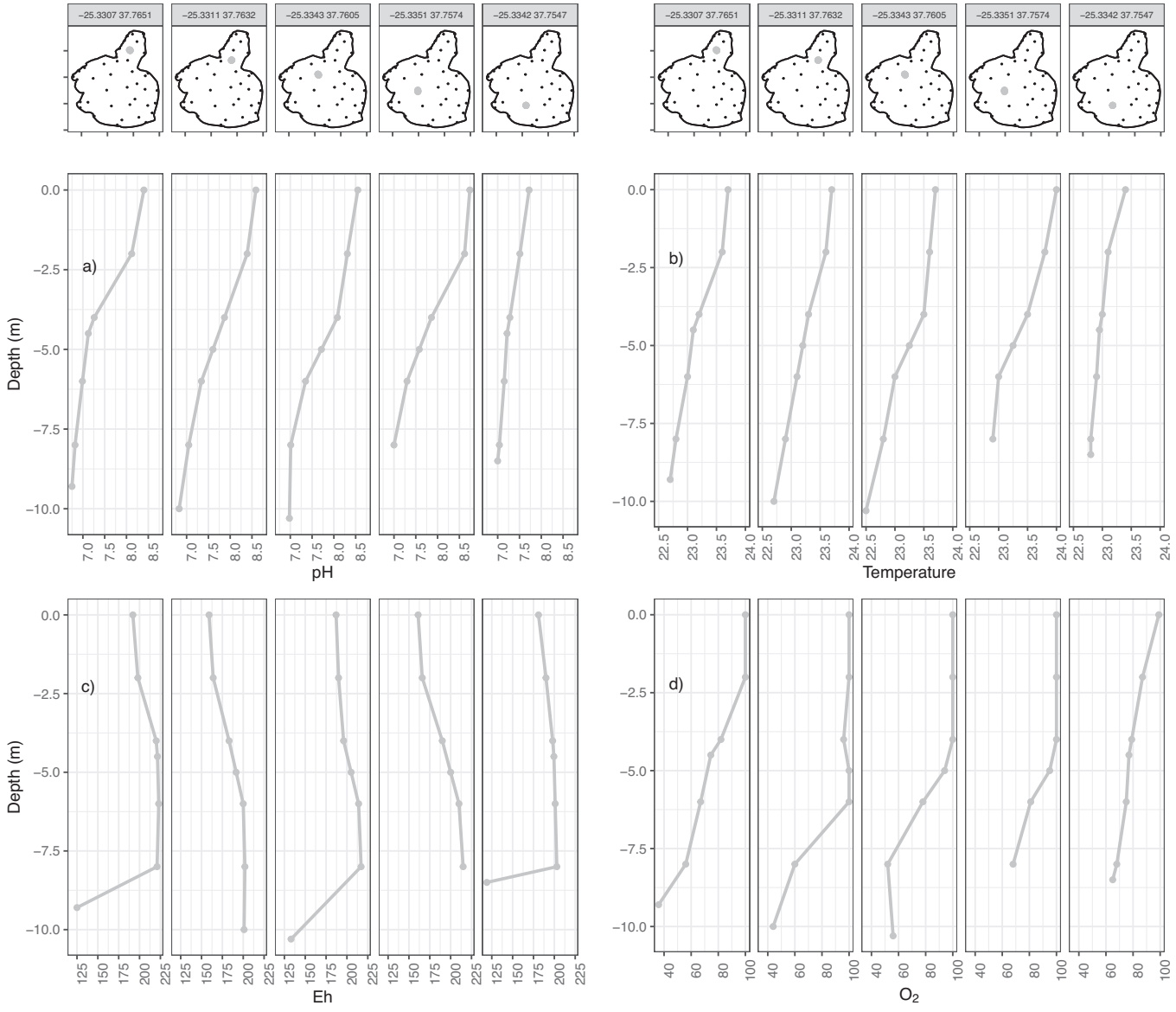

Fig. 2. Vertical profiles of pH, temperature, redox condition and dissolved oxygen at 5 representative sites of Lagoa das Furnas, from north to south.

4. Results and discussion

The measurements were performed during one single field campaign between the 30th of August and the 3rd of September 2021 (summer time). Lake water temperature ranged between 14.4 °C (due to the inflow of a small spring on the western shore) and 27.2 °C (in the northern sector with bubbling fumaroles), and values for pH ranged between 6 and 9.2 (Fig. 1c and 2a). The longitudinal transect at approximately 1-m depth (Fig. 1c and d) shows these end-members' temperature and acidity transition. The vertical profiles along the longitudinal axis of the lake (Fig. 2) show general decreasing (for pH, temperature and dissolved oxygen) and increasing (for Eh) monotonic trends with depth indicating a specific stratification of the lake during the study. At some sites, the bottom water layer shows a sudden variation of the redox state toward more reducing conditions (lower Eh values) and low dissolved oxygen concentrations, probably pointing to the degradation of organic matter accumulated at the bottom of the lake (Bastviken et al., 2004; Woszczyk et al., 2011). Dissolved $CO_{2(aq)}$ ranged between 0.14 and 122 mg·L^{-1} (Fig. 1e). The maximum concentrations are found in the northern bubbling sites at ~1 m depth. At higher depths, in the central and southern sectors of the lake, $CO_{2(aq)}$ increases up to ~50 mg·L^{-1} near the bottom. The dissolved $CO_{2(aq)}$ reported in the literature (Cruz et al., 2006; Andrade et al., 2016; Melián et al., 2017) range from 1.5 to 28.8 mg·L^{-1}. We find good agreement with the previous values if we exclude our measurements carried out in the intensely bubbling sites (0.15–43 mg·L^{-1} below a latitude of 37°45′43″).

After the injection of fumarolic $CO_{2(g)}$ in the water, two subsequent reactions occur:

$$CO_{2(g)} \leftrightarrow CO_{2(aq)} \quad (4)$$

$$CO_{2(aq)} + H_2O \leftrightarrow HCO_3^- + H^+ \quad (5)$$

Reaction 5 is pH-dependent. At the measured pH range (6–9.2), the dissolved inorganic carbon (DIC) is present as $CO_{2(aq)}$, HCO_3^- and CO_3^{2-}. $CO_{2(aq)}$ concentrations increase for pH < 7.5 (see red circles in Fig. 3a). The relationship between $CO_{2(aq)}$ and pH depends on the total alkalinity (TA in mg·L^{-1} of HCO_3^-) given that, for the same CO_2 input, high TA values tends to buffer the subsequent drop of pH (i.e. shown by more vertical dotted lines at high TA in Fig. 3a). Given the long operational times to sample every measurement point for its TA detection, and within the scope to provide of a snapshot view (days long) of the dissolved CO_2 content in the lake, we here used our measured pH and $CO_{2(aq)}$ concentrations to calculate TA values at shallow, midpoint, and bottom depths reached with both the CO_2 and pH probes. This has provided us with a lower and upper TA to be used to calculate a range of $CO_{2(aq),\,CALC}$ concentrations for the intermediate depths covered only by pH measurements (every 2 m of depth per profile, see the sketch diagram in Fig. 4). In order to carry out these calculations, we used *AquaEnv* (Hofmann et al., 2010), an integrated R software package for aquatic chemical model generation that can describe pH, related CO_2 air–water exchange, as well as aquatic acid–base chemistry in general for marine, estuarine or freshwater systems. Both the calculated ranges ($CO_{2(aq),\,CALC}$) and directly measured ($CO_{2(aq),\,MEAS}$) values of dissolved CO_2 are shown in Fig. 3a. It is evident that the buffer capacity of the TA (and thus

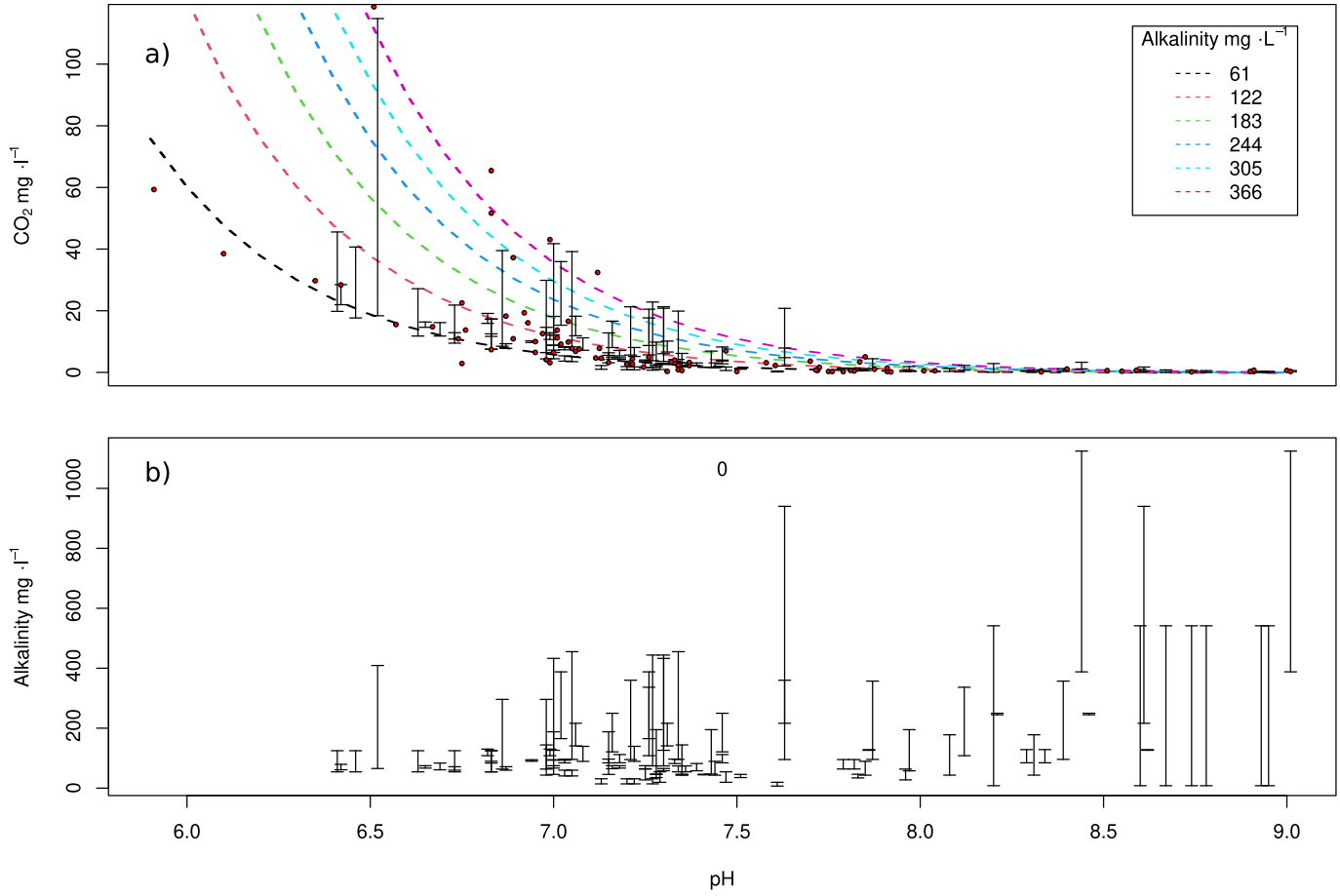

Fig. 3. a) Measured concentrations of dissolved $CO_{2(aq)}$ VS measured pH (red circles). The values are compared with the calculated $CO_{2(aq)}$ concentrations at different pH and alkalinity values obtained with AquaEnv (colored dashed lines). The vertical black segments show the calculated upper and lower $CO_{2(aq)}$ concentrations obtained by combining the measured $CO_{2(aq)}$ and pH with the b) calculated total alkanity with AquaEnv (see text for explanation and Fig. 4). (For interpretation of the references to colour in this figure legend, the reader is referred to the web version of this article.)

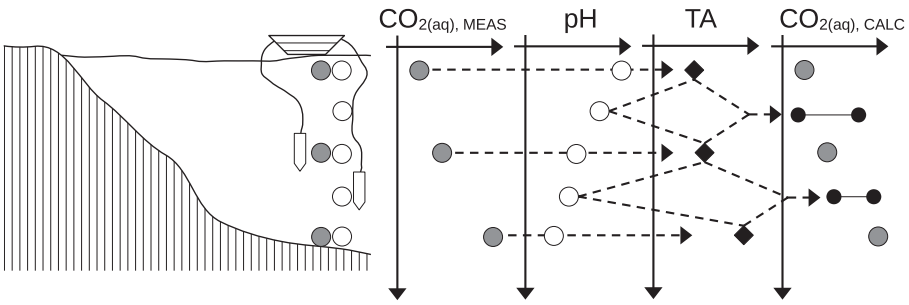

Fig. 4. Diagram sketching the operations followed to calculate a range of $CO_{2(aq),\ CALC}$ concentrations for each measured pH value between the measured $CO_{2(aq),\ MEAS}$ concentrations.

its controlling role) is relevant for pH < 7.5. Therefore, we obtained a lower and upper estimates of the spatial distribution of $CO_{2(aq)}$ concentrations at Lagoa das Furnas. The $CO_{2(aq)}$ concentrations (both lower and upper estimates) at each depth have subsequently been spatially interpolated using multilevel B-splines (Lee et al., 1997; Finley et al., 2017). We chose this methodology because of the low density of the grid points (not suitable for a variogram model) and because it reproduces the smooth spatial variations of water physicochemical parameters. For the interpolation, we used the *mba.surf* function of the *MBA* R package (Finley et al., 2017) set with a 100 × 100 grid (corresponding to a cell size of 15.18 m × 20.12 m) and five levels in the hierarchical construction. We added complementary interpolations among the measured depth layers considering the points of both the upper and bottom layers (e.g. interpolation at 3 m of depth using the measurements at 2 and 4 m). These complementary interpolations also provided a vertically smoothened variability and decreased the noise. As a result, the lake is divided into a discrete three-dimensional grid of voxels (with a voxel of 15.18 m × 20.12 m × 1 m) for a total volume of $1.5{\cdot}10^7$ m^3 (as estimated by Andrade et al., 2021).

The total $CO_{2(aq)}$ mass stored in the lake is eventually obtained by summing the $CO_{2(aq)}$ masses from each individual voxel. Our calculation yields a total dissolved $CO_{2(aq)}$ ranging from ~109 to ~176 tons (Fig. 5a-b). For comparison, Lake Monoun and Lake Nyos accumulated prior to and released during their limnic eruptions ~26,000 and ~ 650,000 tons of CO_2 in the mid-80s, respectively (Kusakabe, 2015). We argue that the amount of CO_2 stored in Lagoa das Furnas unlikely threatens the local population. This result is not surprising since Lagoa das Furnas misses the three essential requirements (well summarised by Kling et al., 2015) that can lead to a serious CO_2 accumulation: i) being deep and large enough to contain a substantial amount of CO_2 in solution and at high pressures; ii) being strongly stratified for many years to allow gas accumulation and avoid gas-discharge during annual turn-over; iii) having a substantial input of CO_2 at depth.

Our estimate of the total $CO_{2(aq)}$ stored in the lake allows us to infer the residence time of CO_2 in the lake if the out flux is known. In summer (i.e. the period of this campaign), when lake stratification is more stable and hence CO_2 storage capacity is higher, low CO_2 fluxes (i.e. 52 t d^{-1}) were measured by Andrade et al. (2016). Considering a CO_2 content of 109–176 tons and given the reasonable assumption of continuous resupply of CO_2 from rising bubbles or waters with higher contents of $CO_{2(aq)}$, the residence time of CO_2 in the lake in summer ranges from 2 to 3.4 days. The latter are minimum estimates given the buffering capacity of HCO_3^- that can convert to $CO_{2(aq)}$, which then keeps degassing. In addition, HCO_3^- contributes to the total carbon stored in the lake. If we consider for each voxel an amount of CO_2 dissolved as HCO_3^- ranging from 46.4 to 64.7 mg·L^{-1} (measured by Cruz et al., 2006 and Andrade et al., 2019), we obtain an equivalent CO_2 mass of 502–700 tons for Lagoa das Furnas. However, the water pH values at Furnas, especially in the shallow water layers (up to 9.2), suggest that a certain amount of carbon can also be stored as CO_3^{2-}. There are no available estimates of CO_3^{2-} in the literature. Hence, we used the direct pH measurements and the already estimated range of alkalinity to calculate with *AquaEnv* (Hofmann et al., 2010) the CO_3^{2-} concentrations and interpolate the values across the lake volume following the same procedure adopted for $CO_{2(aq)}$ (see supplementary material). The CO_3^{2-} concentrations follow an inverse spatial distribution than the $CO_{2(aq)}$ (Fig. 1S), with higher concentrations in the shallower and less acidic layers and very low concentrations in the deeper and more acidic layers. If we sum the interpolated CO_3^{2-} concentrations across the whole lake, we obtain an equivalent amount of CO_2 of 130–190 tons. Hence, the total carbon stored in the lake would range between 741 and 1066 equivalent tons of CO_2 during our observation period.

The 3D mapping of the $CO_{2(aq)}$ in Lagoa das Furnas reveals its heterogeneous distribution across the lake's volume (Fig. 5b-c), which is also an effect of the more stable summer stratification. Such characteristics would be hardly observable with few vertical profiles as commonly used to study volcanic lakes (Tassi and Rouwet, 2014). We found a ubiquitous accumulation of CO_2 at the bottom of the lake, probably due to the contribution of both organic degradation and volcanic degassing. We can better discriminate those sources at shallower depths, where the volcanic contribution creates rising plumes of dissolved CO_2 (Fig. 5d-g) that are visible in correspondence with the identified fumarolic flares (yellow asterisks in Fig. 5a, Melián et al., 2017) and the diffusive CO_2 degassing at the water-air interface (Fig. 5a, Andrade et al., 2016). Such rising plumes reach shallower depths if we consider the upper limit (Fig. 5g) of the TA range used to calculate the $CO_{2(aq)}$ at different pH values.

We argue that such plumes reach the surface only when the degassing at the bottom of the lake is strong enough (purple triangle in Fig. 5d-g) or the lake is shallow enough (bubbling sites in the northern sector). When the degassing is weak, the CO_2 probably dissipates by dissolution before reaching the surface (green diamond in Fig. 5d-g). The weak degassing of the latter site is also demonstrated by the lack of an evident surface anomaly by Andrade et al. (2016). These deep degassing structures, only detectable through our 3D tomography, are aligned along the WNW-ESE direction, in agreement with the tectonic structures observed in the Furnas caldera rims (Fig. 1b, Guest et al., 2015; Carmo, 2013).

5. Conclusions

This study investigated the physicochemical dynamics of Lagoa das Furnas during a summer field campaign in 2021. The lake exhibited varied temperature, pH, and dissolved oxygen levels, indicating a distinct stratification. Dissolved CO_2 concentrations ranged widely, with higher values in the northern sector associated to fumaroles. The spatial

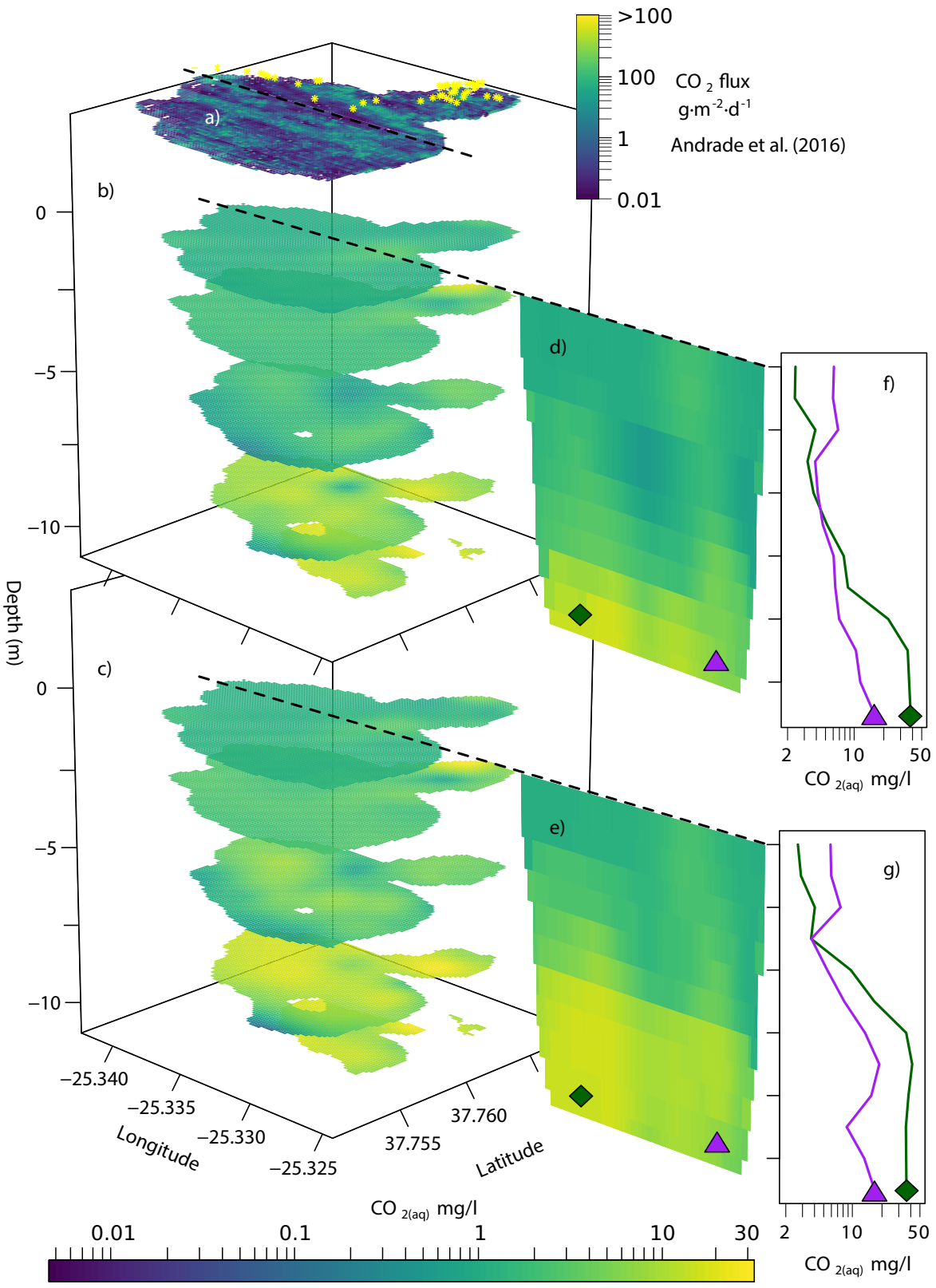

Fig. 5. Comparison between multiple cross-sections of the $CO_{2(aq)}$ values calculated for Lagoa das Furnas and the a) diffusive CO_2 degassing obtained by Andrade et al. (2016) in March 2014 and the position of the fumarolic flares (yellow asterisks) from Melián et al. (2017). The diffusive CO_2 map is shown higher up for ease of reading, but it must be considered as it was at the surface of the lake. The estimated b) lower and c) upper $CO_{2(aq)}$ concentrations at different depths (−1, −3, −6, −9, −11 m) are shown with the corresponding vertical cross-sections (d-e) across two $CO_{2(aq)}$ plumes (green diamond and purple triangle) and the plots of the vertical profiles (e-f). (For interpretation of the references to colour in this figure legend, the reader is referred to the web version of this article.)

distribution of $CO_{2(aq)}$ concentrations revealed heterogeneity across the lake, with accumulation at the bottom attributed to organic degradation and volcanic degassing. Total $CO_{2(aq)}$ mass was estimated at 109 to 176 tons (741–1024 tons of CO_2 if we consider the contribution of HCO_3^- and CO_3^{2-}), posing no significant threat to the local population due to the lake lacking crucial conditions for serious CO_2 accumulation. The research highlighted the importance of 3D mapping for accurate CO_2 distribution depiction, offering insights into rising plumes at shallower depths. We suggest applying the same 3D chemical tomography to other degassing volcanic lakes, as the distribution of dissolved CO_2 in volcanic lakes might be less homogeneously distributed than previously thought, especially for shallow, and poorly stratified or overturning lakes.

Author agreement statement

We declare that this manuscript is original, has not been published before and is not currently being considered for publication elsewhere.

We confirm that the manuscript has been read and approved by all named authors and that there are no other persons who satisfied the criteria for authorship but are not listed. We further confirm that the order of authors listed in the manuscript has been approved by all of us. We understand that the Corresponding Author is the sole contact for the Editorial process.

CRediT authorship contribution statement

Giancarlo Tamburello: Conceptualization, Data curation, Formal analysis, Funding acquisition, Investigation, Methodology, Project administration, Resources, Software, Supervision, Validation, Visualization, Writing – original draft, Writing – review & editing. **Dmitri Rouwet:** Conceptualization, Investigation, Methodology, Writing – review & editing. **César Andrade:** Investigation, Methodology, Writing – review & editing. **Fátima Viveiros:** Investigation, Methodology, Supervision, Writing – review & editing. **J. Virgílio Cruz:** Investigation, Supervision, Writing – review & editing.

Declaration of competing interest

The authors declare the following financial interests/personal relationships which may be considered as potential competing interests.

Giancarlo Tamburello reports administrative support, equipment, drugs, or supplies, and travel were provided by EU Framework Programme for Research and Innovation Research Infrastructures and *E*-Infrastructures. If there are other authors, they declare that they have no known competing financial interests or personal relationships that could have appeared to influence the work reported in this paper.

Data availability

Furnas Lake measured and calculated data is accessible through the Figshare open research data repository (10.6084/m9.figshare.22794110).

Acknowledgements

The research leading to these results was funded by the EUROVOLC project (grant agreement 731070, H2020-EU.1.4) through a proposal named “3DCO2 AZORES” submitted to the EUROVOLC 2nd call for Transnational Access (https://eurovolc.eu/?p=1483).

Appendix A. Supplementary data

Supplementary data to this article can be found online at https://doi.org/10.1016/j.jvolgeores.2024.108012.

References

Andrade, C., Viveiros, F., Cruz, J.V., Coutinho, R., Silva, C., 2016. Estimation of the CO_2 flux from Furnas volcanic Lake (São Miguel, Azores). J. Volcanol. Geotherm. Res. 315, 51–64. https://doi.org/10.1016/j.jvolgeores.2016.02.005.

Andrade, C., Viveiros, F., Cruz, J.V., Branco, R., Moreno, L., Silva, C., Pacheco, J., 2019. Diffuse CO_2 flux emission in two maar crater lakes from São Miguel Island (Azores, Portugal). J. Volcanol. Geotherm. Res. 369, 188–202. https://doi.org/10.1016/j.jvolgeores.2018.11.030.

Andrade, C., Viveiros, F., Cruz, J.V., Coutinho, R., 2021. Global Carbon Dioxide output of Volcanic Lakes in the Azores Archipelago, Portugal. J. Geochem. Explor. 229, 106835 https://doi.org/10.1016/j.gexplo.2021.106835.

Bastviken, D., Persson, L., Odham, G., Tranvik, L., 2004. Degradation of dissolved organic matter in oxic and anoxic lake water. Limnol. Oceanogr. 49 (1), 109–116.

Battaglia, A., de Moor, M.J., Aiuppa, A., et al., 2019. Insights into the mechanisms of phreatic eruptions from continuous high frequency volcanic gas monitoring: Rincón de la Vieja Volcano, Costa Rica. Front. Earth Sci. https://doi.org/10.2289/feart.2018.00247.

Brumberg, H.D., Capece, L., Cauley, C.N., Tartell, P., Smith, C., Wagner, M.S., Varekamp, J.C., 2021. Volcanic carbon cycling in East Lake, Newberry Volcano, Oregon, USA. Geology 49 (6), 718–722. https://doi.org/10.1130/G48388.1.

Caliro, S., Viveiros, F., Chiodini, G., Ferreira, T., 2015. Gas geochemistry of hydrothermal fluids of the S. Miguel and Terceira Islands, Azores. Geochim. Cosmochim. Acta 168, 43–57. https://doi.org/10.1016/j.gca.2015.07.009.

Carmo, R., 2013. Estudos de Neotectónica na ilha de S. Miguel, Uma Contribuição Para o Estudo do Risco Sísmico no Arquipélago dos Açores. PhD Thesis. Universidade dos Açores, Ponta Delgada (in Portuguese with English abstract 381 p.).

Carmo, R., Madeira, J., Ferreira, T., Queiroz, G., Hipólito, A., 2015. Volcano-tectonic structures of S. Miguel Island, Azores. In: Gaspar, J.L., Guest, J.E., Duncan, A.M., Barriga, F.J.A.S., Chester, D.K. (Eds.), Volcanic Geology of São Miguel Island (Azores Archipelago), 44. Geological Society of London Memoir, pp. 65–86. https://doi.org/10.1144/M44.6.

Caudron, C., Mazot, A., Bernard, A., 2012. Carbon dioxide dynamics in Kelud volcanic lake. J. Geophys. Res. 117 https://doi.org/10.1029/2011JB008806 (B05102).

Caudron, C., Campion, R., Rouwet, D., Lecocq, T., Capaccioni, B., Syahbana, D., Bernard, A., 2017. Stratification at the Earth's largest hyperacid lake and its consequences. Earth Planet. Sci. Lett. 459, 28–35. https://doi.org/10.1016/j.epsl.2016.11.002.

Chiodini, G., Tassi, F., Caliro, S., Chiarabba, C., Vaselli, O., Rouwet, D., 2012. Time-dependent CO2 variations in Lake Albano associated with seismic activity. Bull. Volcanol. 74, 861–871. https://doi.org/10.1007/s00445-011-0573-x.

Cruz, J.V., Antunes, P., Amaral, C., França, Z., Nunes, J.C., 2006. Volcanic lakes of the Azores archipelago (Portugal): Geological setting and geochemical characterization. J. Volcanol. Geotherm. Res. 156 (1–2), 135–157. https://doi.org/10.1016/j.jvolgeores.2006.03.008.

de Moor, J.M., Aiuppa, A., Pacheco, J., Avard, G., Kern, C., Liuzzo, M., Martínez, M., Giudice, G., Fischer, T.P., 2016. Short-period volcanic gas precursors to phreatic eruptions: insights from Poa´s volcano, Costa Rica. Earth Planet. Sci. Lett. 442, 218–227. https://doi.org/10.1016/j. epsl.2016.02.056.

Finley, A., Banerjee, S., Hjelle, Ø., 2017. MBA: Multilevel B-Spline Approximation, R Package Version 0.0–9. https://CRAN.R-project.org/package=MBA.

Guest, J.E., Pacheco, J.M., Cole, P.D., Duncan, A.M., Wallenstein, N., Queiroz, G., Gaspar, J.L., Ferreira, T., 2015. The volcanic history of Furnas volcano, São Miguel, Azores. In: Gaspar, J.L., Guest, J.E., Duncan, A.M., Barriga, F.J., Chester, D.K. (Eds.), Volcanic Geology of São Miguel Island (Azores Archipelago), 44. Geological Society of London Memoir, pp. 125–134.

Gunawan, H., et al., 2017. New insights into Kawah Ijen's volcanic system from the wet volcano workshop experiment. In: Ohba, T., Capaccioni, B., Caudron, C. (Eds.), Geochemistry and Geophysics of Active Volcanic Lakes, 437. Geological Society of London, Special Publications. https://doi.org/10.1144/SP437.7.

Herczeg, A.L., Fairbanks, R.G., 1987. Anomalous carbon isotope fractionation between atmospheric CO_2 and dissolved inorganic carbon induced by intense photosynthesis. Geochim. Cosmochim. Acta 51 (4), 895–899.

Hernández, P.A., Melián, G.V., Somoza, L., Arpa, M.C., Pérez, N.M., Bariso, E., et al., 2017. The Acid Crater lake of Taal Volcano, Philippines: Hydrogeochemical and Hydroacoustic Data Related to the 2010-11 Volcanic Unrest. In: Ohba, T., Capaccioni, B., Caudron, C. (Eds.), Geochemistry and Geophysics of Active Volcanic Lakes, 437. Geological Society of London, Special Publications, pp. 131–152. https://doi.org/10.1144/SP437.17.

Hernández, P.A., Nogami, K., Padrón, E., Somoza, L., Amonte, C., Mori, T., Melián, G.V., Sumino, H., Kikawada, Y., Pérez, N.M., 2021. Hydrochemical and Hydroacoustic Investigation of the Yugama Acid Crater Lake, Kusatsu-Shirane, Japan. Front. Earth Sci. 9, 741795 https://doi.org/10.3389/feart.2021.741795.

Hofmann, A.F., Soetaert, K., Middelburg, J.J., Meysman, F., 2010. AquaEnv : An Aquatic Acid–Base Modelling Environment in R. Aquat. Geochem. 16, 507–546. https://doi.org/10.1007/s10498-009-9084-1.

Jácome-Paz, M.P., Taran, Y., Inguaggiato, S., Collard, N., 2015. CO_2 flux and chemistry of El Chi- chón crater lake (Mexico) in the period 2013–2015: evidence for enhanced volcano activity. Geophys. Res. Lett. https://doi.org/10.1002/2015GL066354.

Jolie, E., 2019. Detecting gas-rich hydrothermal vents in volcanic lakes with hazard potential for CO_2 bursts. Nat. Sci. Rep. https://doi.org/10.1038/s41598-019-48576-5.

Kling, G.W., Clark, M.A., Compton, H.R., Devine, J.D., Evans, W.C., Humphrey, A.M., Koenigsberg, E.J., Lockwood, J.P., Tuttle, M.L., Wagner, G.N., 1987. The 1986 Lake Nyos gas disaster in Cameroon, West Africa. Science 236, 169–175.

Kling, G.W., Evans, W.C., Tanyileke, G.Z., 2015. The Comparative Limnology of Lakes Nyos and Monoun, Cameroon. In: Rouwet, D., Christenson, B., Tassi, F., Vandemeulebrouck, J. (Eds.), Volcanic Lakes. Advances in Volcanology. Springer-Verlag, Berlin-Heidelberg. https://doi.org/10.1007/978-3-642-36833-2_1.

Kusakabe, M., 2015. Evolution of CO_2 Content in Lakes Nyos and Monoun, and Sub-Lacustrine CO_2 Recharge System at Lake Nyos as Envisaged from $CO_2/^3He$ Ratios and Noble Gas Signatures. In: Rouwet, D., Christenson, B., Tassi, F., Vandemeulebrouck, J. (Eds.), Volcanic Lakes, Advances in Volcanology. Springer-Verlag, Berlin-Heidelberg, pp. 427–450. https://doi.org/10.1007/978-3-642-36833-2_19.

Kusakabe, M., 2017. Lake Nyos and Monoun gas disasters (Cameroon)–Limnic eruptions caused by excessive accumulation of magmatic CO_2 in crater lakes. Geochem. Monograph Series 1 (1), 1–50. https://doi.org/10.5047/gems.2017.00101.0001.

Lee, S., Wolberg, G., Shin, S.Y., 1997. Scattered data interpolation with multilevel B-splines. IEEE Trans. Vis. Comput. Graph. 3 (3), 229–244.

Mazot, A., Rouwet, D., Taran, Y., Inguaggiato, S., Varley, N., 2011. CO_2 and he degassing at El Chichón volcano (Chiapas, Mexico): gas flux, origin and relationship with local and regional tectonics. Bull. Volcanol. 73, 423–441. https://doi.org/10.1007/s00445-010-0443-y.

Melián, G., Somoza, L., Padrón, E., Pérez, N.M., Hernández, P.A., Sumino, H., Forjaz, V. H., França, Z., 2017. Surface CO_2 emission and rising bubble plumes from degassing of crater lakes in São Miguel Island, Azores. Geol. Soc. Spec. Publ. 437 (1), 233–252. https://doi.org/10.1144/SP437.14.

Melián, G.V., Toulkeridis, T., Pérez, N.M., Hernández, P.A., Somoza, L., Padrón, E., Amonte, C., Alonso, M., Asensio-Ramos, M., Cordero, M., 2021. Geochemistry of Water and Gas Emissions from Cuicocha and Quilotoa Volcanic Lakes, Ecuador. Front. Earth Sci. 9, 741528 https://doi.org/10.3389/feart.2021.741528.

Pérez, N.M., Hernández, P.A., Padilla, G., Nolasco, D., Barrancos, J., Melían, G., et al., 2011. Global CO_2 Emission from Volcanic Lakes. Geology 39 (3), 235–238. https://doi.org/10.1130/G31586.1.

Rouwet, D., 2021. Volcanic lake dynamics and related hazards. Chapter 11. In: Papale, P. (Ed.), Forecasting and Planning for Volcanic Hazards, risks, and disasters. Elsevier, pp. 439–471. https://doi.org/10.1016/B978-0-12-818082-2.00011-1.

Rouwet, D., Tassi, F., Mora-Amador, R., Sandri, L., Chiarini, V., 2014. Past, present and future of volcanic lake monitoring. J. Volcanol. Geotherm. Res. 272, 78–97. https://doi.org/10.1016/j.jvolgeores.2013.12.009.

Shinohara, H., Yoshikawa, S., Miyabuchi, Y., 2015. Degassing activity of a volcanic crater lake: Volcanic plume measurements at the Yudamari crater lake, Aso volcano, Japan. In: Rouwet, D., Christenson, B.W., Tassi, F., Vandemeulebrouck, J. (Eds.), Volcanic Lakes. In: Advances of Vol- Canology IAVCEI Series. Springer, Heidelberg. https://doi.org/10.1007/978-3-642-36833-2_8.

Sigurdsson, H., Devine, J.D., Tchoua, F.M., Presser, T.S., Pringle, M.K.W., Evans, W.C., 1987. Origin of the lethal gas burst from Lake Monoun, Cameroun. J. Volcanol. Geotherm. Res. 31, 1–16.

Tamburello, G., et al., 2015. Intense magmatic degassing through the lake of Copahue volcano, 2013-2014. J. Geophys. Res. https://doi.org/10.1002/2015JB012160.

Tassi, F., Rouwet, D., 2014. An overview of the structure, hazards, and methods of investigation of Nyos-type lake from the geochemical perspective. J. Limnol. 73 (1) https://doi.org/10.4081/jlimnol.2014.836.

Viveiros, F., Cardellini, C., Ferreira, T., Caliro, S., Chiodini, G., Silva, C., 2010. Soil CO_2 emissions at Furnas Volcano, São Miguel Island, Azores archipelago: volcano monitoring perspectives, geomorphologic studies, and land use planning application. J. Geophys. Res. 115 (B12), B12208. https://doi.org/10.1029/2010JB007555.

Weiss, R.F., 1974. Carbon dioxide in water and seawater: the solubility of a nonideal gas. Mar. Chem. 2, 203–215. https://doi.org/10.1016/0304-4203(74)90015-2.

Woszczyk, M., Bechtel, A., Cieśliński, R., 2011. Interactions between microbial degradation of sedimentary organic matter and Lake hydrodynamics in shallow water bodies: insights from Lake Sarbsko (northern Poland). J. Limnol. 70 (2), 293.